Excitation of CO_2 by energy transfer from highly vibrationally excited benzene derivatives

Beatriz M. Toselli[a] and John R. Barker
Department of Atmospheric, Oceanic, and Space Sciences, Department of Chemistry, Space Physics Research Laboratory, The University of Michigan, Ann Arbor, Michigan 48109-2143

(Received 29 July 1991; accepted 27 August 1991)

The time-resolved infrared fluorescence technique has been used to study V–V and V–T/R energy transfer to carbon dioxide from highly excited benzene, benzene-d_6, toluene, and toluene-d_8. The highly vibrationally excited aromatics in the electronic ground state are obtained by radiationless transitions after pumping with a KrF laser at 248 nm to the S_1 excited electronic level. The V–V energy transfer from the excited parent to the asymmetric stretch mode of CO_2 was measured by observing the characteristic emission of CO_2^* near 4.3 μm. From these measurements, the probability per collision of formation of CO_2^* was determined as a function of the internal energy in the excited aromatic. In all cases investigated, this probability is $\leq 0.1\%$ at the initial excitation energy of 40 000 cm^{-1} and it is approximately directly proportional to the vibrational energy of the excited aromatic. The total concentration of CO_2^* produced as a result of the many collisions needed to totally deactivate the excited aromatic amounted to $> 5\%$ of the initial concentration of the excited aromatic and the quantitative values obtained are in excellent agreement with other work. A simple dipole–dipole interaction model is shown to explain the observed magnitude of V–V energy transfer and it is used to predict the amount of energy transferred to the bending mode of CO_2. A key feature of this model is that the states of the highly vibrationally excited polyatomic are assumed to be broadened by rapid intramolecular vibrational redistribution of energy. In addition to the V–V energy-transfer measurements, the average energy lost per collision by the excited aromatic was determined as a function of the vibrational energy of the aromatic, and the rate constants were determined for CO_2^* deactivation by the nondeuterated species. For the deuterated species, the results implicated a contribution from resonant V–V transfer between the C–D stretch modes and the asymmetric stretch mode of CO_2. The overall results for the CO_2 collider gas indicate that V–V energy transfer contributes a relatively small portion of the total energy transfer, and that portion can be described with the dipole–dipole interactions model.

I. INTRODUCTION

Energy transfer in highly excited polyatomic molecules has been studied for many years, but a detailed understanding of the important mechanisms is still far from complete. Several experimental techniques have been used to study energy transfer in mid-sized and large polyatomic molecules. The time-resolved infrared fluorescence technique (IRF) technique has been used to measure the average energy transferred per collision in collisions of various collider gases with several excited molecules: azulene,[1,2] 1,1,2-trifluoroethane,[3] benzene,[4] toluene,[5] and toluene-d_8.[6] The time-dependent thermal lensing technique has recently been used to study energy transfer from NO_2 to the rare gases[7] and experiments using excited CS_2 are currently underway in this laboratory. Deactivation by the rare gases is an example of vibration to translation/rotation (V–T/R) energy transfer (the rotations and translations are tightly coupled, and it is not possible to distinguish them in these experiments). Troe and co-workers have used the ultraviolet absorption technique to follow the collisional deactivation of several molecules, including azulene,[8] some benzene derivatives,[9] CS_2,[10] and SO_2.[11] They have also used a multiphoton photoexcitation method in competition with a chemical isomerization reaction to obtain information about energy transfer at very high excitation energies.[12] Weston and co-workers[13,14] used the infrared tunable diode laser (TDL) absorption technique to study energy transfer in several systems. The TDL technique is particularly useful in studies of vibration to vibration (V–V) energy transfer, because it probes directly the population of selected rovibrational states.

Previously, experiments were carried out in which the IRF from excited CO_2 (ν_3, asymmetric stretch mode) was observed as a result of V–V transfer from highly vibrationally excited azulene.[1,15] By measuring the emission intensity of CO_2^* near 4.3 μm relative to emission from the azulene C–H stretch modes near 3.3 μm, the yield of CO_2^* was estimated. These measurements indicated that V–V energy transfer between excited azulene and the asymmetric stretch mode of CO_2 is not very efficient. It was also shown that a major fraction of the emission originates from difference bands that include the ν_3 mode of CO_2. These were the first experi-

[a] Present address: Atomic Energy of Canada Limited Research, Chalk River Laboratories, Chalk River, Ontario, Canada, K0J 1J0.

 0021-9606/91/238108-12$03.00

mental measurements that showed that vibrational excitation of the bath gas occurs as the result of the deactivation of large molecules. Jalenak *et al.*[13] used the TDL absorption technique to confirm the early measurements on highly excited azulene and they extended them to azulene-d_8. They found considerable excitation in the CO_2^* bending mode and the total vibrational energy transferred to CO_2 was determined to be ~25% of the initial azulene energy. In other recent experiments, Flynn and co-workers[14] used the TDL technique to investigate V–V energy transfer to CO_2, CO, and N_2O from highly excited NO_2. For these three collider gases, they found that only a small fraction of the available energy is transferred to the ν_3 modes of CO_2 and N_2O and to the $v = 1$ level of CO. While the present paper was in preparation, we learned that Sedlacek, Weston, and Flynn[16] also used the TDL method to study V–V energy transfer to ν_3 of CO_2 from excited C_6H_6, C_6D_6, and C_6F_6 and the results again show that V–V transfer is relatively inefficient.

In the present work, the IRF technique has been used to monitor the V–V energy transfer to ν_3 of CO_2 from excited benzene, benzene-d_6, toluene, and toluene-d_8. The experimental results are in excellent agreement with those of Sedlacek, Weston, and Flynn, and they have been used to extract the probability of V–V energy transfer per collision as a function of the average vibrational energy of the excited aromatic. In addition, a simple theoretical model is developed which is capable of describing quantitatively the energy-dependent V–V energy-transfer probability. A key feature of this model is that the states of the excited polyatomic are assumed to be broadened by rapid intramolecular vibrational redistribution of energy (IVR).

II. EXPERIMENT

Experiments were carried out using the IRF technique, which has been described elsewhere.[4] Basically, a KrF excimer laser (248 nm) irradiated the gas-phase species in a 30 cm long, 4.5 cm diam Pyrex cell. IRF was viewed through a quartz side window (to monitor the C–H emission near 3.3 μm) or through a CaF_2 side window (to monitor the C–D emission and/or the CO_2 (001) spontaneous emission near 4.3 μm) with a 3 mm diam 77 K InSb photovoltaic detector (Infrared Associates) equipped with a matched preamplifier and appropriate interference filters. In the experiments designed to measure the deactivation of the excited parent by CO_2, the pressure of parent was held constant at 10 mTorr and the CO_2 pressure was varied from 50 to 300 mTorr. The experiments designed to measure the production of CO_2^* and its subsequent deactivation were performed under static bulb conditions in mixtures containing 30–70 mTorr of benzene or its derivatives ("parent" gas) and 10 and 20 mTorr of CO_2. The CO_2 pressures were kept low to avoid self-absorption by the strongly absorbing CO_2 in the ~3 cm pathlength between the emission volume and the window of the cell.[17]

The detector signals were amplified with a Tektronix AM 502 ac-coupled amplifier and averaged with a LeCroy 9400 digital oscilloscope for ~5000 pulses, in order to achieve good signal-to-noise (S/N) ratios in each experiment. The signal was further analyzed after transfer to a Macintosh personal computer. The IRF signals were limited by the ~5 μs rise time of the infrared detector/preamplifier. Laser-beam transmittance measurements gave absorption cross sections (base e) of $(3.6 \pm 0.2) \times 10^{-19}$ cm^2 for toluene-d_8, $(3.5 \pm 0.2) \times 10^{-19}$ cm^2 for benzene-d_6, and $(3.7 \pm 0.2) \times 10^{-19}$ cm^2 for both toluene-d_0 and benzene-d_0. The laser fluence employed in the present measurements was ~25 mJ cm^{-2} per shot, so that approximately 0.5% of the molecules in the laser beam were excited. It was shown in earlier experiments[4,5] that the quantum yield for photodissociation of these aromatics at 248 nm is of the order of 5%, but this is not expected to cause problems in the present experiments, because the fragments will carry little excitation energy and will not emit significantly, as explained elsewhere.[5]

Toluene-d_8 (Sigma, 99 + at. % D), benzene-d_6 (Aldrich, 99.5 + at. % D), benzene (Fisher Scientific, ACS grade), and toluene (Aldrich) were degassed prior to use. The CO_2 (Air Products, research grade) was used without further purification.

III. RESULTS AND DISCUSSION

A. Deactivation of the excited parent by CO_2

To investigate the deactivation of the excited parent by CO_2, IRF experiments were performed in which the pressure of the parent was kept constant while the CO_2 pressure was varied. For benzene-d_0 and toluene-d_0, we monitored the decay in the IRF signal near 3050 cm^{-1} (~3.3 μm), which corresponds to the C–H stretch modes. The intensity of the emission is related to the energy residing in the excited aromatic and thus the intensity decay corresponds to the energy decay due to collisional deactivation. Emission from the ν_3 mode of CO_2 near 2349 cm^{-1} (~4.3 μm) is not transmitted by the 3 μm bandpass filter and causes no interference. The experimental IRF decay curves were fitted by nonlinear least squares to the empirical time-dependent function used in previous work,[4,5]

$$\langle\langle I(t)\rangle\rangle = I_P^* \exp(-k^I t + b^I t^2) + B, \tag{1}$$

where I_P^* is the initial intensity of the C–H or C–D stretching-mode fundamental emission, k^I and b^I are pseudo-first-order parameters, and B is the nominal background intensity. The double angular brackets indicate that the observed IRF corresponds to the bulk average over the population distribution, which evolves with time.

In order to relate the observed IRF signal to the vibrational energy content of the excited toluene, the following theoretical expression[18] was used:

$$I(E) = \frac{N_{ex}}{\rho_s(E)} \sum_{i=1}^{\text{modes}} h\nu_i A_i^{1,0} \sum_{v_i=1}^{v_{\max}} v_i \rho_{s-1}(E - v_i h\nu_i). \tag{2}$$

Here, N_{ex} is the number of vibrationally excited molecules, $A_i^{1,0}$ is the Einstein coefficient for spontaneous emission for the $0 \leftarrow 1$ transition of mode i, v_i is its quantum number, $h\nu_i$ is the energy of the emitted photon, and $\rho_s(E)$ and $\rho_{s-1}(E - v_i h\nu_i)$ are, respectively, the density of states for all s oscillators at energy E and that for the $s-1$ modes,

TABLE I. Data for collisions with CO_2.

Excited molecule	$10^{10}k_{LJ}$ [a] ($cm^3\ s^{-1}$)	$-\langle\langle\Delta E\rangle\rangle_{inv}$ [b,c] (cm^{-1})	$\langle\Delta E\rangle_d = C_0 + C_1E + C_2E^2$		
			C_0 (cm^{-1})	C_1	10^7C_2 ($1/cm^{-1}$)
C_6H_6	4.93	208 ± 4	47.7[d]	0.0202[d]	-3.11[d]
C_7H_8	5.46	245 ± 6	37.4[e]	0.0230[e]	-3.33[e]
C_6D_6	4.45	...	...	...	...
C_7D_8	5.39	...	...	...	...

[a] Calculated using Lennard-Jones parameters from Refs. 4 and 9.
[b] Uncertainties are $\pm 2\sigma$ statistical errors; possible systematic errors are not included.
[c] Evaluated at $\langle\langle E\rangle\rangle_{inv} = 24\,000\ cm^{-1}$.
[d] From Ref. 5.
[e] Whitten–Rabinovitch parameters for toluene (see Ref. 5 for notation), based on vibrational assignment from Ref. 20: $E_z = 27\,109.0\ cm^{-1}$, $\beta = 1.3644$, $s = 38$, $r = 1$.

omitting the emitting mode and the energy contained in it. The summations are carried out for all vibrational modes that emit in the wavelength range observed and for all vibrational levels of each mode permitted by conservation of energy.

Equation (2) was used with vibrational assignments[19–22] for the excited molecules to calculate $I(E)$ "calibration curves," as described elsewhere,[4,5] which relate vibrational energy to the observed IRF intensity. These curves were used to invert the IRF data to give the bulk average energy $\langle\langle E(t)\rangle\rangle_{inv}$ and the bulk average energy transferred per collision $\langle\langle\Delta E\rangle\rangle_{inv}$, using the procedure described elsewhere.[4,5] The results of this analysis are plots $\langle\langle\Delta E\rangle\rangle_{inv}$ as a function of $\langle\langle E\rangle\rangle_{inv}$ for each experimental run, which is characterized by a mixing ratio of parent/collider. Note that only the product $k_{LJ}\cdot\langle\langle\Delta E\rangle\rangle_{inv}$ is determined from the experiments and the value of $\langle\langle\Delta E\rangle\rangle$ is inferred by assuming Lennard-Jones parameters for the calculation of k_{LJ} (Table I).

As in other recent work, $\langle\langle\Delta E\rangle\rangle$, the bulk-average energy transferred per collision was obtained by extrapolating the collision fraction of collider to unity.[5] The collision fraction is the fraction of collisions due to parent–collider gas interactions,

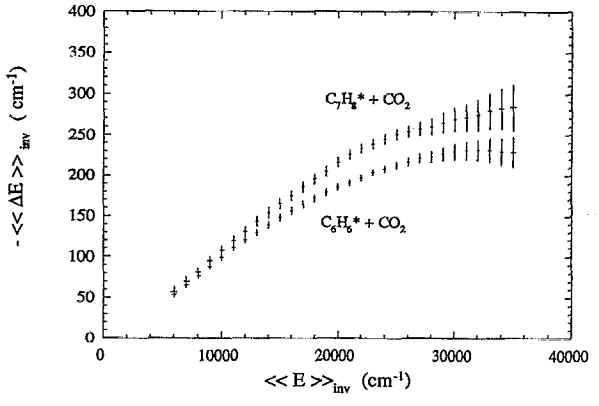

FIG. 1. $-\langle\langle\Delta E\rangle\rangle_{inv}$ vs $\langle\langle E\rangle\rangle_{inv}$ for deactivation of excited toluene-d_0 and benzene-d_0 by CO_2. The error bars are $\pm 2\sigma$ statistical uncertainties.

$$\text{Collision fraction} = F_c = \frac{[CO_2]k^c_{LJ}}{[CO_2]k^c_{LJ} + [P]k^p_{LJ}}. \quad (3)$$

Here, the square brackets denote concentrations and k^p_{LJ} and k^c_{LJ} and are bimolecular collision rate constants for the excited parent in collisions with the unexcited parent and with the collider (CO_2), respectively, calculated using Lennard-Jones parameters.

The values of $\langle\langle\Delta E\rangle\rangle_{inv}$ for CO_2 ($F_c = 1$) deactivation of C_6H_6 and C_7H_8 are presented in Fig. 1; these new results are in excellent agreement with the data reported earlier for these species.[4,5] As in our recent work on excited toluene,[5] the $\langle\langle\Delta E\rangle\rangle_{inv}$ vs $\langle\langle E\rangle\rangle_{inv}$ data were least-squares fitted to obtain coefficients describing $\langle\Delta E\rangle_d$, the microcanonical energy transferred in deactivating collisions (down steps); the results are presented in Table I. The results for $\langle\Delta E\rangle_d$ can be used with the formulas in Ref. 5 to obtain quantitative expressions for $\langle\langle\Delta E\rangle\rangle_{inv}$ vs $\langle\langle E\rangle\rangle_{inv}$, or they can be used to implement master-equation simulations. For the deuterated molecules, it was not possible to determine $\langle\langle\Delta E\rangle\rangle_{inv}$ for parent + CO_2 collisions, because the CO_2 emission at 2349 cm^{-1} interferes with the emission from the C–D modes at $\sim$2300 cm^{-1} and an unambiguous analysis of the IRF signal from the parent was not possible at the high pressures of CO_2 required for the deactivation study.

B. Formation of CO_2^*

The rate of production of excited CO_2 was monitored by observing the spontaneous emission of the asymmetric stretch mode (ν_3) isolated with a bandpass filter near 4.3 μm. The actual states of the excited CO_2 cannot be identified from these measurements, except that the 4.3 μm band is associated with $\Delta v_3 = -1$. Thus we will designate the excited species as CO_2^*. There is some evidence in the azulene + CO_2 system that two or more vibrational modes of CO_2 can be excited simultaneously,[1,15] but there is no direct evidence that more than one quantum resides in ν_3, which has a relatively high vibrational frequency. Thus, the CO_2^* probably can be identified with $CO_2(v_1v_2 1)$, where

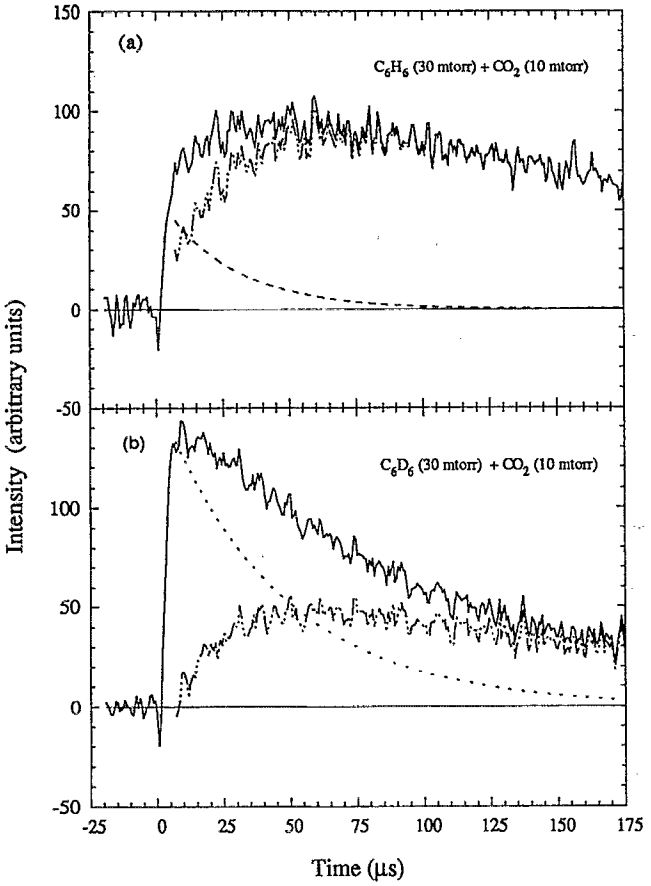

FIG. 2. Infrared fluorescence observed near 4.3 μm for 248 nm excitation of benzene-d_0 or benzene-d_6 mixed with CO_2. The solid line represents the actual measured intensity and the dashed lines show the contribution to the total intensity from CO_2^* and excited parent emissions.

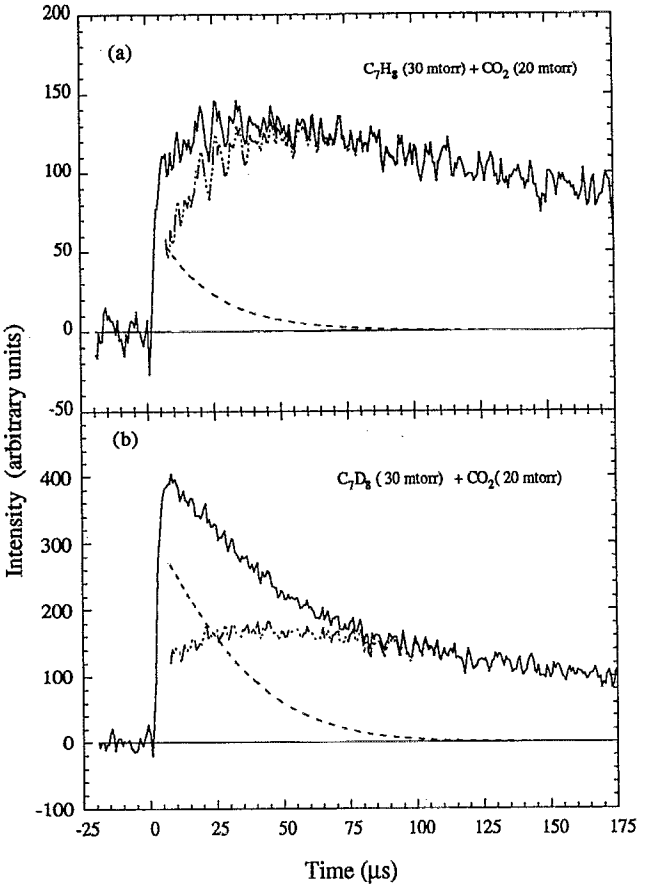

FIG. 3. The same as Fig. 2, but for toluene-d_0 and toluene-d_8.

$v_1, v_2 \geqslant 0$. The analysis of the results is not affected, however, even if v_3 is greater than unity.

In all of the experiments aimed at measuring the production of CO_2^*, the CO_2 pressure was kept low for two reasons: (1) to avoid complications due to self-absorption[17] of the 4.3 μm IRF by CO_2, and (2) to allow the collisional deactivation of excited parent (P^*) to be dominated by $P^* + P$ collisions, rather than $P^* + CO_2$ collisions. Because energy transfer by $P^* + P$ collisions for the benzene and toluene systems has been investigated previously,[4-6] as well as in the present study, it is possible to infer the rate of CO_2^* production corresponding to a specified bulk average energy of P^*.

The CO_2^* emission was isolated with an interference filter that also transmitted some of the emission from the C–D stretching vibrations. In the case of the benzene-d_0 or toluene-d_0, the total emission measured through the interference filter was mostly due to CO_2^*, although there was a small IRF intensity due to the emission of the excited parent. Typical signals observed near 4.3 μm for benzene–CO_2 and toluene–CO_2 are shown in Figs. 2(a) and 3(a), respectively. The results obtained with the two excited nondeuterated species are similar, although the production of CO_2^* is not as great for toluene-d_0, as shown in Fig. 4. In the case of the deuterated species, the analysis of the IRF signal is complicated due to the presence of strong emission from the C–D stretching modes near $\sim 2300\ cm^{-1}$, as shown in Figs. 2(b) and 3(b) for C_6D_6–CO_2 and C_7D_8–CO_2, respectively. In each figure are shown the contributions to the 4.3 μm IRF from the excited parent and from CO_2^*.

It should be noted that Sedlacek, Weston, and Flynn[16] discovered that multiphoton ionization of benzene yielded low-energy electrons, which produced vibrational excitation in the CO_2 collider gas, when the laser fluence was in the

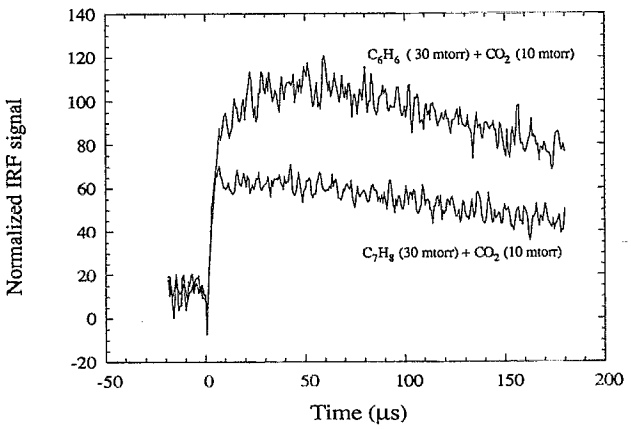

FIG. 4. Comparison of the normalized IRF intensity at 4.3 μm for benzene-d_0 and toluene-d_0.

range used in the present study. In their study, however, the partial pressures of the parent were lower than those used here and it is likely that the aromatic moderates the superthermal electrons, reducing the yield of excited CO_2^*, which would appear "instantaneously" on the time scale of the present experiments. Although the data are limited by the rise time of the infrared detector, there is no indication of prompt CO_2^* production in the present experiments (see below).

Each of the IRF intensity decay curves in Figs. 2 and 3 is characterized by a detector-limited rapid rise, often followed by a more gradual rise to a maximum, followed by a slower decay. For the deuterated compounds, a maximum is not observed and the final decay is on a very long time scale. The general features of this behavior can be explained as the sum of contributions at 4.3 μm from the excited parent and from CO_2^*. For convenience in the analysis, the IRF signals were fitted using the Marquardt nonlinear least-squares algorithm[23] to the following empirical function:

$$\langle\langle I(t)\rangle\rangle = I_A[1-\exp(-k_a t)]\exp(-k_b t) + I_P\exp(-k_c t). \quad (4)$$

This descriptive empirical function can be rationalized by the following simplified mechanism:

$$P^{**}+P\rightarrow 2P, \quad (5)$$

$$P^{**}+CO_2\rightarrow P+CO_2, \quad (6a)$$

$$P^{**}+CO_2\rightarrow P+CO_2^*, \quad (6b)$$

$$CO_2^*+P\rightarrow CO_2+P, \quad (7a)$$

$$CO_2^*+P\rightarrow CO_2+P^*, \quad (7b)$$

$$CO_2^*+CO_2\rightarrow 2CO_2, \quad (8)$$

$$CO_2+P^*\rightarrow CO_2^*+P, \quad (9a)$$

$$CO_2+P^*\rightarrow CO_2+P, \quad (9b)$$

$$P^*+P\rightarrow 2P. \quad (10)$$

Here, P, P^*, and P^{**} represent parent molecules with no excitation, a small amount of excitation, and high excitation, respectively. For deuterated molecules, both P^{**} and P^* can emit strongly near 4.3 μm. The highly excited parent is deactivated in collisions with unexcited parent and with CO_2. Some of the $P^{**}+CO_2$ collisions produce CO_2^*, which, in turn, is deactivated in collisions with unexcited parent and very slowly[14] by CO_2. In the case of the deuterated species, some of the CO_2^*+P collisions produce P^* with one quantum of excitation in the C–D stretching modes according to reaction (7b), perhaps due to resonant V–V energy transfer. The reverse reaction is also possible, and may be rapid, leading to a quasiequilibrium and a very slow decay of the fluorescence, which is due to both P^* and CO_2^* emitting near 4.3 μm; reactions (7a), (8), (9b), and (10) are responsible for the very slow decay.

Using reactions (5)–(8) for the nondeuterated species and the initial conditions that the concentration of P^{**} is $[P^{**}]_0$ and that $[CO_2^*]_0=[P^*]_0=0$, the CO_2^* concentration as a function of time is found to be

$$[CO_2^*]=\frac{k_{6b}[CO_2][P^{**}]_0}{\{(k_5-k_7)[P]+(k_6-k_8)[CO_2]\}} \times[1-\exp(-t\{(k_5-k_7)[P]+(k_6-k_8)[CO_2]\})] \times\exp(-t\{k_7[P]+k_8[CO_2]\}). \quad (11)$$

Equation (11) has the same form as the first term of the empirical equation (4). Thus, the empirical pseudo-first-order rate constants can be identified as $k_a=\{(k_5-k_7)[P]+(k_6-k_8)[CO_2]\}$ and $k_b=\{k_7[P]+k_8[CO_2]\}$. The second term in Eq. (4) is proportional to $[P^{**}]$, which is given by

$$[P^{**}]=[P^{**}]_0\exp(-t\{k_5[P]+k_6[CO_2]\}), \quad (12)$$

TABLE II. Experimental conditions and data for the production of CO_2^*.

Excited molecule	Parent (mTorr)	CO_2 (mTorr)	$10^{-4}k_a$ (s^{-1})	$10^{-4}k_c$ (s^{-1})	$\frac{I_P^*(3.3 \text{ or } 4.3\ \mu m)}{I_A(4.3\ \mu m)}$
C_6H_6	30	10	3.48	3.57	7.19[a]
C_6H_6	40	10	4.26	4.66	8.91[a]
C_6H_6	50	10	5.79	5.75	8.76[a]
C_7H_8	30	10	3.62	4.48	15.34[a]
C_7H_8	40	10	5.55	5.86	20.90[a]
C_7H_8	50	10	6.94	7.23	34.61[a]
C_6D_6	30	10	1.74	2.01	1.60
C_6D_6	40	10	2.31	2.58	2.65
C_6D_6	50	10	4.14	3.16	2.90
C_7D_8	30	10	4.89	3.14	2.31
C_7D_8	40	10	9.34	4.02	3.11
C_7D_8	50	10	>10	4.89	...

[a] Ratio of observed intensities multiplied by 1.15 to include the detector response and filter transmittance.

and thus we would expect $k_c \approx k_a$ when $k_5 \gg k_7$ and $k_6 \gg k_8$. For three of the molecules investigated (excepting toluene-d_8), the rising portion of the signal (after the detector-limited rise time) is fitted with a value for k_a that is very similar to k_c (Table II). This result is in agreement with results found by Jalenak *et al.*[13] and by Sedlacek, Weston, and Flynn,[16] who used the tunable diode laser absorption technique to study several aromatics in collisions with CO_2.

It must be emphasized that the mechanism given above is greatly simplified and that the rate constants are phenomenological and do not correspond to elementary processes. Nonetheless, the mechanism can be used to rationalize the use of Eq. (4) in describing the observed IRF at 4.3 μm.

C. Rate of deactivation of CO_2^* by the unexcited parent

The CO_2^* is deactivated only very slowly by unexcited CO_2,[14] and so the long decay is due to diffusion and to collisional deactivation by the parent molecule (Figs. 2 and 3). In a series of experiments, the pressure of the aromatics was varied between 30 and 70 mTorr for two pressures of CO_2 (10 and 20 mTorr). The 4.3 μm IRF signal (due to mostly CO_2^* emission in nondeuterated systems, and due to both the C–D stretches of the aromatic and the CO_2^* in the deuterated systems) was fitted by least squares to a double-exponential function. The IRF was observed using a long time scale and the least-squares fits included only the data corresponding to the time subsequent to CO_2^* formation.

In collisions with benzene-d_0 and with toluene-d_0, it was found that the observed CO_2^* fluorescence decays are fitted well by a single exponential and the first-order decay rate constants were found to be nearly proportional to the pressure of the aromatic, as shown in Fig. 5 for toluene. The corresponding bimolecular rate constants are $k_b(\text{benzene} + CO_2^*) = (2.99 \pm 0.34) \times 10^{-12}$ cm^3 s^{-1}, and $k_b(\text{toluene} + CO_2^*) = (3.48 \pm 0.10) \times 10^{-12}$ cm^3 s^{-1} (uncertainties are $\pm 1\sigma$). These values were obtained by weighted linear least squares of the first-order rate constants as a function of $[P]$, with the intercept constrained to 351 s^{-1}, which is the radiative lifetime of CO_2 (001).[24]

In collisions with the deuterated aromatics, the CO_2^* fluorescence decays were also well described by a single-exponential function, but they were much slower than observed with the nondeuterated species. Furthermore, the first-order decay rate constants actually *decrease* with increasing $[P]$, as shown in Fig. 5 for toluene-d_8. This behavior may indicate that the fluorescence decay is primarily due to diffusion from the field of view of the detector, or to the walls where deactivation can occur. This hypothesis was tested by calculating a diffusion rate given by $1/\tau_d$ where τ_d is the characteristic time for diffusion in one dimension,

$$\tau_d = x^2/2D. \tag{13}$$

Here, D is the binary diffusion coefficient ($\sim 7.054 \times 10^{-2}$ cm^2 s^{-1} at 1 atm), and x is the distance, estimated to be 1.25 cm for the geometry of our experiments. The resulting decay constants are shown as the solid curved line in Fig. 5, and it is in excellent agreement with the experimental data. Thus we conclude that the rate of collisional deactivation in the deuterated case is negligible, unlike the nondeuterated case.

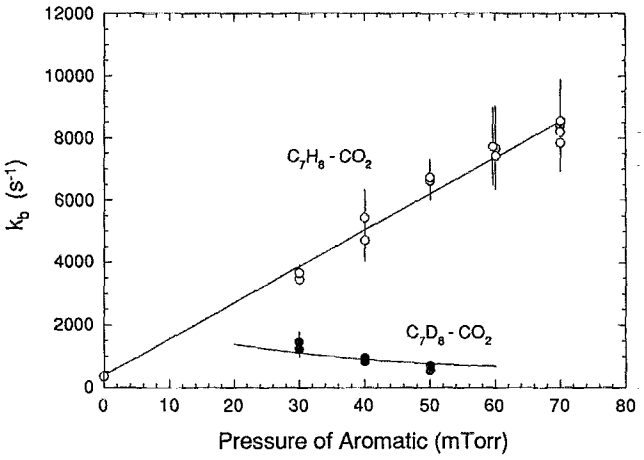

FIG. 5. The deactivation of CO_2^* by unexcited toluene or toluene-d_8. The results for toluene-d_8 are almost completely controlled by diffusion (see text for details).

The difference in behavior between the deuterated and the nondeuterated molecules may be due to reversible near-resonant energy transfer between the ν_3 mode of CO_2 (2349 cm^{-1}) and the C–D stretching modes (~ 2300 cm^{-1}) in the deuterated aromatics, as expressed by reactions (7b) and (9a). For the deuterated species, the reactions that deactivate CO_2^* and P^* must be much slower than the characteristic time scale for diffusion. There are six or more C–D modes in each aromatic in equilibrium with the ν_3 mode in CO_2, if rapid equilibrium is maintained between CO_2^* and P^*; this implies that $[P^*]/[CO_2^*] \geqslant 6$ and much of the IRF near 4.3 μm may be due to P^*, in addition to CO_2^*. Deactivation of the fluorescence may correspond to deactivation of either CO_2^*, or P^*: TDL experiments or high-resolution IRF measurements could distinguish between these two possibilities.

In the nondeuterated cases, the resonant energy transfer is not possible, because these species have no fundamental vibrational frequencies within hundreds of wave numbers of 2349 cm^{-1}. Even if the nondeuterated aromatics retain some residual excitation for time scales longer than diffusion, that energy will not be resonantly transferred to CO_2 and the nondeuterated P^* does not emit strongly within the bandpass of the 4.3 μm filter. Thus, the observed fluorescence decay must correspond to deactivation of CO_2^* by collisions with parent molecules.

D. Probability of CO_2^* formation

The data for the production of CO_2^* are quite consistent, as shown in Fig. 6 for a series of experiments with the benzene + CO_2 system. Similar curves, not shown, were obtained for the other benzene derivatives. The total yield of CO_2^* produced was determined relative to the initial concentration of the excited parent in the following way. The total yield of CO_2^* is proportional to its Einstein coefficient (A_{CO_2}) and its fluorescence intensity near $h\nu_{CO_2} = 2349$ cm^{-1} at very long times, neglecting deactivation of the CO_2^* [I_A from Eq. (4)]. Similarly, the initial concentration of

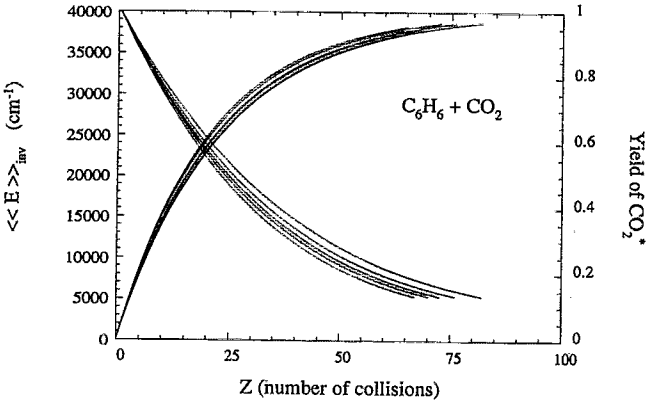

FIG. 6. Production of CO_2^* from collisions with excited benzene-d_0 for several mixtures of benzene (30–50 mTorr) and CO_2 (10 and 20 mTorr). Also shown is the benzene energy decay as a function of the number of collisions.

excited parent is proportional to its Einstein coefficient A_P and the initial intensity I_P^* at $h\nu_P$ (the fundamental of the C–H or C–D stretch modes) as expressed by Eq. (1). Equation (2) can be rewritten as follows for the C–H stretch modes:

$$I_P^* = [P^{**}]_0 \frac{h\nu_P A_P}{\rho_s(E_0)} \sum_{v=1}^{v_{\max}} v\, \rho_{s-1}(E_0 - vh\nu_P), \quad (14)$$

where $E_0 \approx 40\,500\ \mathrm{cm}^{-1}$ (the initial excitation energy of the aromatic), $h\nu_P$ is the emission band frequency of the parent, and A_P is the Einstein coefficient of the whole band for the parent, as given in Table III. Thus, the total concentration of CO_2^* produced, relative to the initial concentration of the excited parent, is

$$\frac{[CO_2^*]_\infty}{[P^{**}]_0} = \frac{I_A}{I_P^*} \frac{h\nu_P A_P}{h\nu_{CO_2} A_{CO_2}} \frac{1}{\rho_s(E_0)} \times \sum_{v=1}^{v_{\max}} v\, \rho_{s-1}(E_0 - vh\nu_P). \quad (15)$$

TABLE III. Einstein A coefficients from infrared active vibrations and model parameters.

Molecule	Band position (cm^{-1})	Upper-state[a] assignment	A[b] (s^{-1})	$10^{-12}\tau_D^{-1}$ (s^{-1})
C_6H_6	3080	ν_{20}	36.3	...
C_6H_6	674	ν_{11}	5.1	0.1
C_6H_6	~2328	$(\nu_{10}+\nu_{19})$, $(\nu_9+\nu_{15})$	~0.25[c]	4
C_6D_6	2287	C–D stretch fundamentals	11.8	2.5
C_7H_8	3056	ν_{20a}	87.9	...
C_7H_8	2341	$(\nu_{8a}+\nu_{11})$	~0.60[c]	1.5
C_7D_8	2284	C–D stretch fundamentals	28.5	~3.3
CO_2	2349	ν_3	351	...
CO_2	667	ν_2	1.35	...

[a] From references for benzene (Ref. 19) benzene-d_6 (Ref. 22), toluene (Ref. 20), and toluene-d_8 (Ref. 21). The lower state is assumed to be the ground state.
[b] Einstein coefficients from Ref. 24, unless otherwise noted.
[c] Estimated from the IR absorption spectra, by comparison with the other bands.

In Eq. (4), the term $I_A[1-\exp(-k_a t)]$ is proportional to the time-dependent concentration of CO_2^* (neglecting its deactivation), which asymptotically approaches $[CO_2]_\infty$. Therefore, the rate of production of CO_2^* is given by the following expression:

$$\frac{d}{dt}[CO_2^*] = [CO_2^*]_\infty k_a \exp(-k_a t). \quad (16)$$

We can also write the rate of production as a bimolecular reaction between P^{**} and CO_2, with the rate constant set equal to the collision rate constant (k_{LJ}^c) multiplied by the probability $Q(t)$ that V–V energy transfer will take place,

$$\frac{d}{dt}[CO_2^*] = Q(t) k_{LJ}^c [CO_2][P^{**}]. \quad (17)$$

In this expression, $[P^{**}]$ is the concentration of excited parent molecules. According to the highly simplified mechanism given above, $[P^{**}]$ varies with time, while the species energy remains fixed. However, in the actual case, $[P^{**}]$ is independent of time and the average energy varies with time during the collisional cascade. Thus, $[P^{**}] = [P^{**}]_0$ at all times and Eqs. (16) and (17) can be combined to obtain the probability for V-V transfer as a function of time,

$$Q(t) = \frac{[CO_2^*]_\infty k_a \exp(-k_a t)}{k_{LJ}^c [CO_2][P^{**}]_0}, \quad (18)$$

This expression is evaluated by using Eq. (15) to determine the ratio $[CO_2^*]_\infty / [P^{**}]_0$. During the time when the CO_2^* is building up, the energy in the excited parent is decaying away,

$$\frac{d}{dt}\langle\langle E\rangle\rangle_m = \{k_{LJ}^c [CO_2] + k_{LJ}^p [P]\}\langle\langle \Delta E\rangle\rangle_m, \quad (19a)$$

$$\frac{d}{dZ}\langle\langle E\rangle\rangle_m = \langle\langle \Delta E\rangle\rangle_m, \quad (19b)$$

where

$$Z = \{k_{LJ}^c [CO_2] + k_{LJ}^p [P]\}t \quad (19c)$$

is the number of collisions and where $\langle\langle E\rangle\rangle_m$ and $\langle\langle \Delta E\rangle\rangle_m$ are the average vibrational energy and the average energy-transfer step size corresponding to the particular mixture of the collider and parent. Thus, at any instant of time, $Q(t)$ is associated with the excitation energy $\langle\langle E\rangle\rangle_m$, thus the probability can be expressed as $Q(E)$, a function of excitation energy. Note that the energy dependence of $Q(E)$ does not depend in any strong way on the particular gas mixture composition or total pressure, which affect only the time dependences of $Q(t)$ and $\langle\langle E\rangle\rangle_m$.

The probabilities obtained from the experimental data using Eq. (18) are shown in Fig. 7 as closely spaced vertical bars of $\pm 1\sigma$ statistical uncertainty. The detailed shapes of the $Q(E)$ curves depend both on the assumed form of the empirical equation (4) (which fits the data well for the non-deuterated species and not as well for the deuterated species) and on the densities of states of the excited parent, according to Eq. (15). In all cases investigated, the probabilities are small, in agreement with other studies,[13–16] which indicate that V–V energy transfer from highly excited molecules is not very efficient when the receptor is a high-frequency vi-

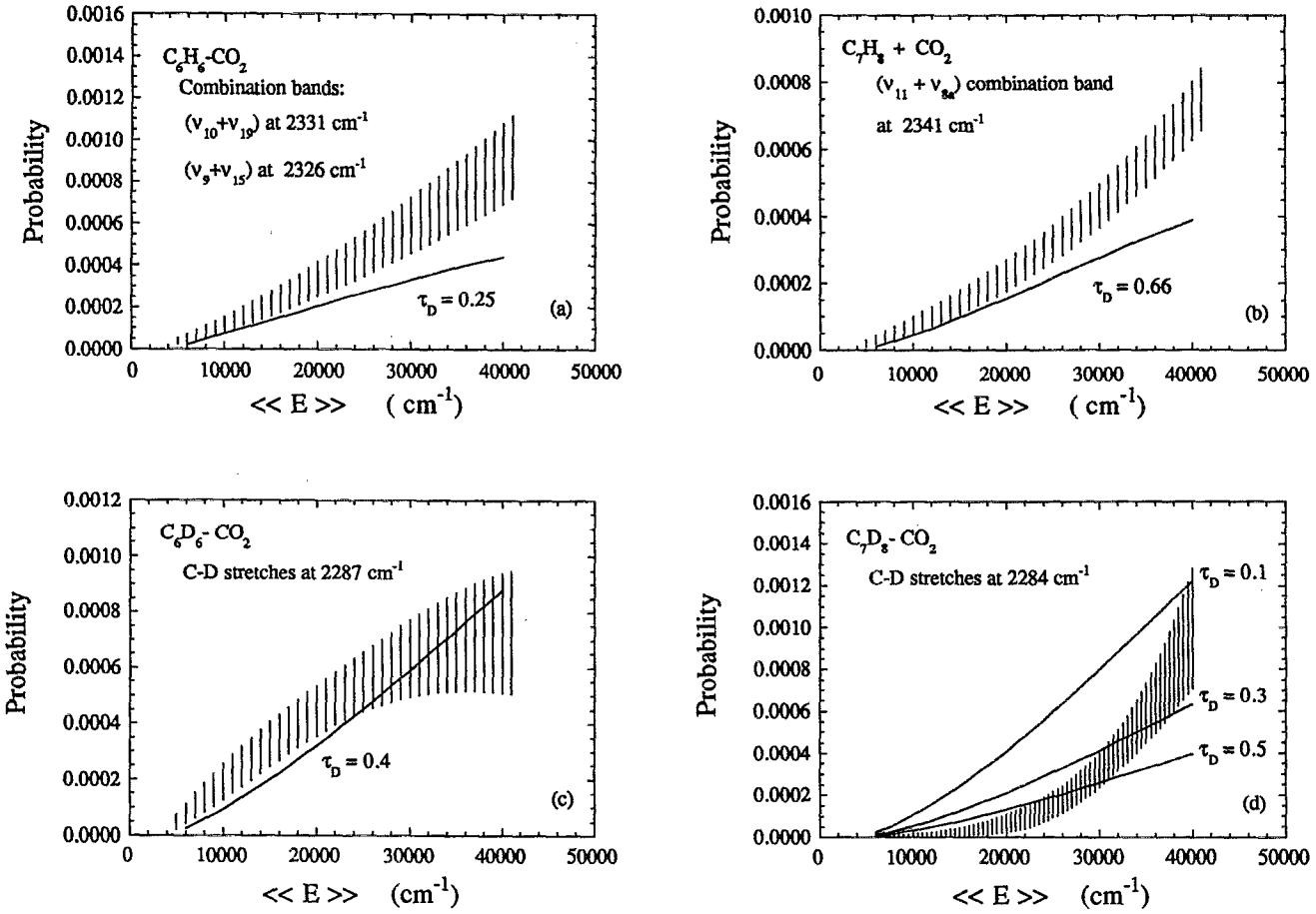

FIG. 7. Experimental and calculated probabilities "per collision" of CO_2^* formation. Also indicated are the IR transitions in the excited polyatomic that make the major contributions to the calculated probabilities. See Table III for model parameters.

bration, like the asymmetric stretch in CO_2.

The $Q(E)$ curves for the nondeuterated species are approximately linear and each may have a small intercept on the energy axis, as expected since $\langle\langle E\rangle\rangle \gtrsim 2349\ \mathrm{cm}^{-1}$ is required for this energy transfer to take place, on the average. For the deuterated species, interference from the C–D stretch-mode emission introduces large uncertainties in the curve fitting which are not reflected by the $\pm 1\sigma$ statistical error bars. We have little confidence in the detailed shapes of the $Q(E)$ curves for the deuterated species, although we are confident the magnitudes are similar to those for the nondeuterated species.

The energy-dependent $Q(E)$ can be used to calculate the ratio $[CO_2^*]_\infty/[P^{**}]_0$ for any mixture of CO_2 and parent, as follows. From Eq. (17), we can write

$$[CO_2^*]_\infty = k_{LJ}^c [CO_2][P^{**}]_0 \int_0^\infty Q(t)dt, \tag{20}$$

which, using Eq. (19a), becomes

$$[CO_2^*]_\infty = \frac{k_{LJ}^c [CO_2][P^{**}]_0}{\{k_{LJ}^c [CO_2] + k_{LJ}^p [P]\}} \times \int_{E_0}^{h\nu_{CO_2}} \frac{Q(E)}{\langle\langle \Delta E\rangle\rangle_m} dE, \tag{21a}$$

$$\frac{[CO_2^*]_\infty}{[P^{**}]_0} = F_c \int_{E_0}^{h\nu_{CO_2}} \frac{Q(E)}{\langle\langle \Delta E\rangle\rangle_m} dE, \tag{21b}$$

where F_c is the collision fraction for the mixture and E_0 is the initial excitation energy.

When $F_c = 1$, $\langle\langle \Delta E\rangle\rangle_m$ corresponds to pure CO_2 and the $[CO_2^*]_\infty/[P^{**}]_0$ ratio in Eq. (21b) corresponds to infinite dilution. For benzene-d_0 and toluene-d_0, the ratios at infinite dilution were found from the present data to be 0.078 ± 0.026 and 0.052 ± 0.017, respectively, where the uncertainties are estimated to be $\pm 33\%$. These results cannot be compared directly with those obtained by Sedlacek, Weston, and Flynn,[16] because those authors obtained their results for a mixture consisting of 20 mTorr of benzene diluted in 80 mTorr of CO_2,[16] where they found $[CO_2^*]_\infty/[P^{**}]_0 = 0.032 \pm 0.011$. By taking the $Q(E)$ determined in the present work and our data for $\langle\langle \Delta E\rangle\rangle_m$ as a function of F_c, we determined $\langle\langle \Delta E\rangle\rangle_m$ for the specific conditions of their experiments and found from Eq. (21b) that $[CO_2^*]_\infty/[P^{**}]_0 = 0.032 \pm 0.011$ for 20 mTorr of benzene diluted in 80 mTorr of CO_2. This result is in excellent agreement with the experimental data of Sedlacek, Weston, and Flynn (the exact numerical agreement is coincidental), and it supports our conclusion that electrons produced by the multiphoton ionization of the aromatic are not con-

tributing significantly to the yield of CO_2^* in the present experiments.

E. Model for the probability of CO_2^* formation

To explain the observed magnitude of the probabilities and to predict the amount of energy transferred to the other vibrational modes of CO_2, we present a simple model based on long-range dipole–dipole interactions. Mahan[25,26] was the first to suggest that long-range electrostatic dipole–dipole interactions could be important for inducing near-resonant V–V energy transfer. Following Yardley,[25] the interaction potential between two dipoles at a distance r is written as

$$V=\frac{\mu_D\mu_A}{r(t)^3}\kappa, \tag{22}$$

where μ_i is the instantaneous dipole moment for the donor ($i=D$) and acceptor ($i=A$), $r(t)$ is the distance between the dipoles, and κ is the angular factor, which varies from $|\kappa|=0$ to $|\kappa|=2$ and is $|\kappa|=(2/3)^{1/2}$ for random orientations. This orientation factor was set equal to unity in the present calculations, because actual orientations are unknown, but may be more favorable than random.[27] Two vibrational states (i,f) can be coupled by electrostatic interactions if the dipole moment derivatives with respect to the vibrational normal coordinate are nonzero for the donor (D) and acceptor (A); the coupling matrix element can be written as

$$V_{if}=\kappa\mu_{ifD}\mu_{ifA}r(t)^{-3}, \tag{23}$$

where μ_{ifD} and μ_{ifA} are the transition matrix elements for dipoles D and A, respectively.

In Förster transfer[28] involving species in viscous solvents, $r(t)$ is independent of time and thus V_{if} is a time-independent perturbation, which is switched on at $t=0$ and switched off at some later time. For the present simple model, we will assume instead that $r(t)$ is described by a straight-line trajectory with constant velocity v and impact parameter b: $r(t)=(b^2+v^2t^2)^{1/2}$. We will also assume that the rate of change of $r(t)$ is sufficiently slow so that V_{if} is suitable for use in Fermi's golden rule for transition probabilities. Following Yardley's discussion[25] of Förster energy transfer, the transition probability per unit time is

$$\frac{dP}{dt}=\frac{8\pi^3}{h^2}[V_{if}(t)]^2\int_{-\infty}^{\infty}g_A(\omega)g_D(\omega)d\omega, \tag{24}$$

where $i=A,D$ and $g_i(\omega)$ is the line-shape function

$$g_i(\omega)=\frac{\tau_i^{-1}}{\pi[\tau_i^{-2}+(\omega-\omega_{if})^2]}, \tag{25}$$

where τ_i is a characteristic time constant. Note that the overlap integral of the absorption and emission line shapes gives a direct measure of the number of states per energy interval coupled by electric dipole matrix elements.[25] Combining Eqs. (23) and (24) and integrating over the trajectory, we find the transition probability,

$$P_{if}(b,v)=K_{if}(\omega)\int_{-\infty}^{\infty}r(t)^{-6}dt, \tag{26}$$

where

$$K_{if}(\omega)=\frac{8\pi^3}{h^2}\mu_{ifD}^2\mu_{ifA}^2\kappa^2\int_{-\infty}^{\infty}g_A(\omega)g_B(\omega)d\omega. \tag{27}$$

This probability is an opacity function which can be used to calculate the cross section for V-V energy transfer,

$$\sigma_{if}(v)=2\pi\int_0^{\infty}P_{if}(b,v)b\,db. \tag{28}$$

Mahan,[26] Sharma and Brau,[29] and Stephenson, Wood, and Moore[30] have described methods to deal with the singularity at $b=0$, and $\sigma_{if}(v)$ is readily evaluated using the Sharma–Brau cutoff at the Lennard-Jones σ_{LJ}. The thermal rate constant for the V–V energy transfer is

$$k_c=\int_0^{\infty}v\sigma_{if}(v)B(T,v)dv, \tag{29}$$

where $B(T)$ is the Maxwell–Boltzmann speed distribution. After some manipulation, the thermal rate constant can be expressed as

$$k_c=\frac{5\pi^2K(\omega)}{8\sigma_{LJ}^3}. \tag{30}$$

Equation (30) was derived as if two isolated dipoles were interacting. In the present system, a CO_2 acceptor dipole interacts with a large molecule, which contains many dipoles and whose vibrational energy is presumed to be rapidly distributed among all vibrational degrees of freedom due to rapid intramolecular vibrational redistribution (IVR). The coupling associated with IVR broadens each vibrational state and it can be characterized by a characteristic lifetime, which we assume is identified with τ_i in the linewidth function. For the large molecule, τ_D is expected to be of the order of 0.1–10 ps, values typical of IVR time constants.[31] For the CO_2 vibrational states, which are not significantly coupled, τ_A is just the natural lifetime, which is very long. Thus, $g_A(\omega)$ can be treated as a delta function, while $g_D(\omega)$ is a Lorentzian with linewidth τ_D. With these assumptions, the integral over ω in Eq. (26) is just equal to $g_D(\omega)$.

The redistribution of energy due to IVR requires that Eq. (30) be multiplied by the probability that the donor mode in the parent contains one or more quanta ($v_D\geqslant 1$). Moreover, the rate constant is proportional to v_D, when harmonic-oscillator wave functions are used to evaluate the matrix elements for fundamentals (slight revisions to the matrix elements are needed for combination bands).[32] If we assume that the energy distribution among the modes in a single molecule is "frozen" just before the collision takes place, the probability of finding v_D quanta in the donor mode can be determined from statistical theory in just the same way as Eq. (2) is derived. Both the scaling with v_D and the statistical factor are included in the following expression for k_c for energy transfer from the vibrational fundamentals of large molecule donors (the expression must be modified slightly for combination bands):

$$k_c=\frac{5\pi^2K(\omega)}{8\sigma_{LJ}^3}\frac{1}{\rho_s(E)}\sum_{v_D=1}^{v_{\max}}v_D\rho_{s-1}(E-v_Dh\nu_D), \tag{31a}$$

$$K(\omega)=\frac{\mu_{ifD}^2\mu_{ifA}^2}{(h/2\pi)^2}\kappa^2g_D(\omega). \tag{31b}$$

For comparison with the experimental data for $Q(E)$, which is expressed on a per-collision basis, we define a calculated probability per collision $Q_c(E)$,

$$Q_c(E) = k_c/k_{LJ}. \tag{32}$$

For a fixed value of τ_D, the probability $Q_c(E)$ decreases very dramatically with the energy mismatch, due to the linewidth function, and the matrix elements are only significant when the energy difference is less than ~ 100 cm^{-1}: near resonance is required.

High-resolution Fourier transform infrared (FTIR) spectra[33] of the benzene derivatives (Fig. 8) were used to identify the transitions that could make a significant contribution to the probability (note that traces of CO_2 in the samples contributed the low-intensity sharp lines seen in the spectra for the aromatics). For toluene-d_8 and benzene-d_6, the bands nearest the CO_2 transition at 2349 cm^{-1} are fundamentals of moderate intensity and, for the purposes of the model calculations, the whole group of fundamentals has been combined into one effective transition with an average frequency. For toluene-d_0 and benzene-d_0, the nearest transitions are combination bands of much weaker intensity. The absorption bands of the aromatics were identified according to the symmetry selection rules for dipole transitions and

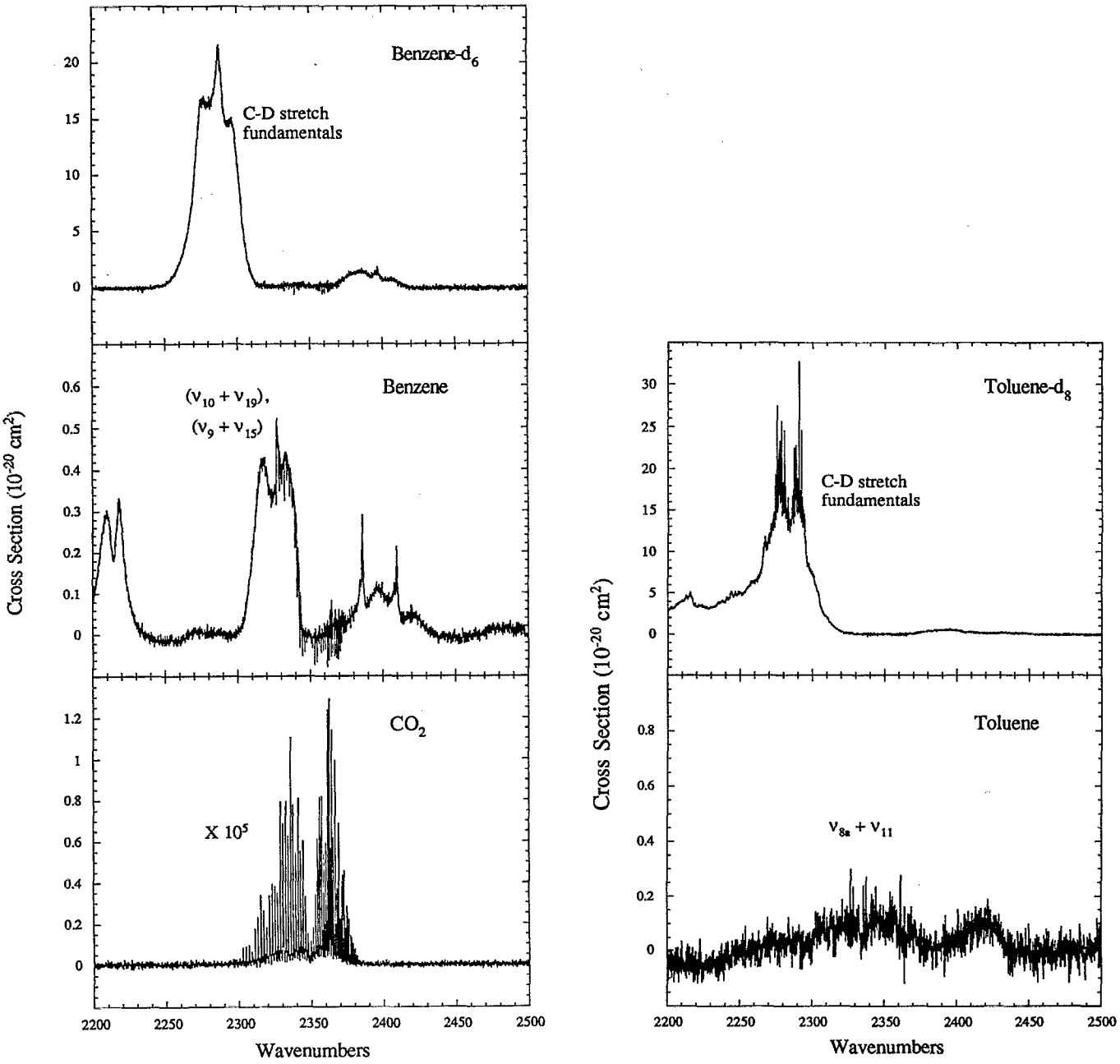

FIG. 8. Infrared absorption spectra of CO_2, benzene-d_0, benzene-d_6, toluene-d_0, and toluene-d_8. The cross sections (base e) were estimated from the measured absorbance, the path length, and the nominal pressure of the absorber, which was diluted in one atmosphere of air. Note that the absorption cross-section scales are different in each panel.

according to band positions. The assignments (Wilson notation) were taken from the literature[19–22] and are presented in Table III. The dipole matrix elements were determined from ratios of integrated band intensities determined from the spectra shown, multiplied by absolute band strengths from the literature, as noted in Table III. The band strength for toluene-d_8 was estimated by assuming that the ratio of Einstein coefficients for toluene-d_8/benzene-d_6 is the same as that for toluene/benzene, since these ratios depend only on the ratios of the dipole transition matrix elements.

The experimental probabilities and those calculated according to this model are presented in Fig. 7. In the calculations, it was assumed that the angular factor $\kappa = 1$, and τ_D was used as an adjustable parameter. It was found that $Q_c(E)$ goes through a maximum as τ_D is varied, due to the normalization and shape of $g(\omega)$, and the best fit (for the nondeuterated molecules) is obtained for the value of τ_D which maximizes $Q_c(E)$; Fig. 9. For the deuterated molecules, τ_D was not chosen at the maximum of the $Q_c(E)$ curve, but was varied to give the best fit. However, the detailed shapes of the experimental curves are not reliable, as discussed above, and not much weight should be placed on the selected values of τ_D. For toluene-d_8, the experimental values are not fitted well by any single value of τ_D, as shown in Fig. 7(d).

As shown in Fig. 7, the agreement between $Q(E)$ and $Q_c(E)$ is good, although $Q_c(E)$ is near the maximum value that this simple model can predict for nondeuterated species. If we had assumed that the dipoles are oriented randomly ($\kappa^2 = 2/3$), the calculated $Q_c(E)$ would have been smaller than the experimental values for nondeuterated species by about a factor of 3. However, there are several factors that may affect the magnitude of $Q_c(E)$, such as the choice of σ_{LJ}. Also, only dipole–dipole attractive interactions were included in the model, although higher-order multipole interactions may contribute. Moreover, only one or two donor modes were considered for each collision pair, although the spectra (Fig. 8) indicate that in some cases other bands fall close enough to 2349 cm^{-1} to make a contribution. Another effect is connected with the rapid IVR, which can take place during the course of the collision: if energy can flow into the donor mode during the collision, the statistical probabilities, which were calculated for "frozen modes," may underestimate the probability of finding a particular vibrational occupation number v_D. It should also be pointed out that anharmonicity may cause the donor mode frequency to shift away from the measured absorption spectrum as the vibrational energy in the molecule is increased, and τ_D may vary with vibrational energy: these effects were neglected.

Despite the limitations of the simple model, the major conclusion is that dipole–dipole interactions appear to explain the V–V energy-transfer process. When trajectory calculations[34,35] and more sophisticated theories[36] are applied to these systems, it will be very important to include dipole–dipole interactions.

Because the simple model gives a good description of the experimental data, calculations were made to predict the amount of vibrational energy transferred to the bending mode of CO_2 (the symmetric stretch is symmetry forbidden) from excited benzene. Benzene has a fundamental band ($\nu_{11} = 674\ cm^{-1}$) in almost exact resonance with the bending mode of CO_2 ($\nu_2 = 667\ cm^{-1}$). The parameters used in this calculation are presented in Table III. The IVR time constant τ_D was estimated on the basis of trajectory calculations reported by Gomez Llorente, Hahn, and Taylor.[37] The dipole–dipole model predicts that much more energy will end up in the bending mode of CO_2 than in the asymmetric stretch. Specifically, the ratio $n^*_{bending}/n^*_{asym} \approx 100$ and V-V energy transfer to the bending mode contributes $\sim 10\%$ of the total $\langle\langle \Delta E \rangle\rangle$, when $E = 40\,000\ cm^{-1}$. The contributions of V–V energy transfer to the CO_2 bend and asymmetric stretch are shown in Fig. 10, along with the experimental measurements of $\langle\langle \Delta E \rangle\rangle_{inv}$. The calculated results are in reasonable agreement with other studies,[13] and the model predicts that V–V energy transfer to the bending mode of CO_2 and V–T/R energy transfer are the two dominant mechanisms. The conclusion that V–T/R energy transfer is probably the most important mechanism for deactivating

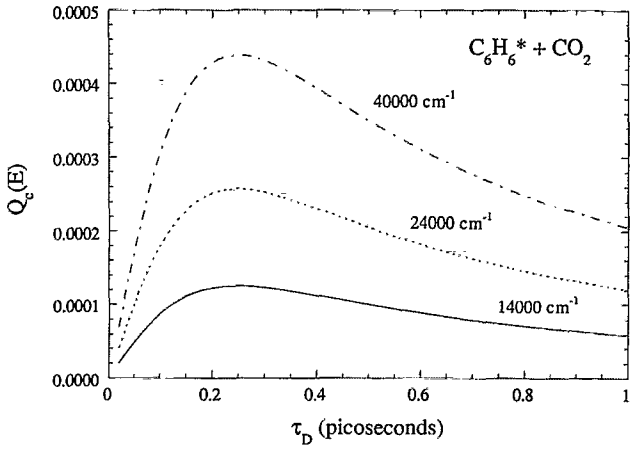

FIG. 9. Calculated probabilities $Q_c(E)$ as a function of τ_D at several vibrational energies for benzene-d_0 + CO_2.

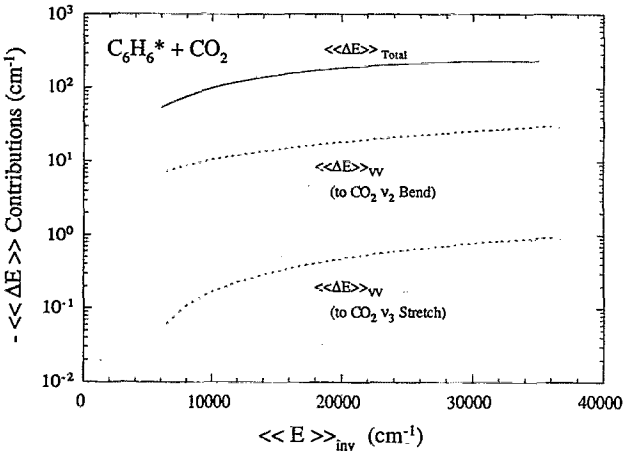

FIG. 10. Estimated contributions of V–V energy transfer to $\langle\langle \Delta E \rangle\rangle_{inv}$ as a function of $\langle\langle E \rangle\rangle_{inv}$ for benzene-d_0 + CO_2.

these highly vibrationally excited species is consistent with the conclusion reached by Lin, Chan, and Rabinovitch[38] some 20 years ago.

IV. CONCLUSIONS

As in our recent papers on benzene[4] and toluene[5] deactivation, the present work is aimed at understanding the mechanisms of large-molecule energy transfer and providing a database for future comparisons with theory. One would expect that the same physical properties that are important for small molecules would also be present in large-molecule energy transfer. Thus it is not surprising that dipole–dipole interactions can explain the extent of V–V energy transfer, as described above, and they must be considered in future theoretical calculations.

In our present view, the collisional deactivation of large molecules can be described with the following components: (1) V–T and V–R energy transfers take place with all colliders, probably due to the repulsive interactions invoked in the biased random walk model[33] (although a classical mechanics description is not quantitatively valid[39]); (2) V–V energy transfer can take place by long-range dipole–dipole interactions, and thus resonance may play a role; (3) if the collider gas has a permanent dipole moment, it is likely that the permanent dipole can interact with the vibrating dipoles of the excited molecule and therefore V–R energy transfer will be enhanced; (4) if low-lying excited electronic states are present, they may enhance energy-transfer rates very substantially.[7]

In the case of collisions with CO_2, V–T/R energy transfer is most likely dominant, but for other systems (parent–parent collisions, in particular) the relative importance of the V–V and V–T/R processes is not yet clear. The third component listed above is a logical extension of the present results and it may explain why polar colliders produce larger $\langle\langle \Delta E \rangle\rangle$ values[40] than nonpolar species of comparable size. If this mechanism is indeed important, energy transfer involving polar collider gases is likely to produce highly excited rotational distributions in the collider gases, which may be observable using time-resolved spectroscopic techniques. Future work in this laboratory will address questions regarding the relative importance of V–V and V–T/R energy transfer, and the possible role of V–R energy transfer involving polar species.

ACKNOWLEDGMENTS

This work was funded by the Department of Energy, Office of Basic Energy Sciences. We thank T. J. Wallington (Ford Motor Company) for generously providing the high-resolution FTIR spectra of the benzene derivatives, and R. E. Weston, Jr., A. J. Sedlacek, and G. W. Flynn for useful discussions and providing a preprint of Ref. 16.

[1] M. J. Rossi, J. R. Pladziewicz, and J. R. Barker, J. Chem. Phys. **78**, 6695 (1983), and references therein; J. R. Barker, J. Phys. Chem. **88**, 11 (1984); J. R. Barker and R. E. Golden, J. Phys. Chem. **88**, 1012 (1984).

[2] J. Shi and J. R. Barker, J. Chem. Phys. **88**, 6219 (1988); J. Shi, D. Bernfeld, and J. R. Barker, *ibid.* **88**, 6211 (1988).

[3] J. M. Zellweger, T. C. Brown, and J. R. Barker, J. Chem. Phys. **83**, 6261 (1985).

[4] M. L. Yerram, J. D. Brenner, K. D. King, and J. R. Barker, J. Phys. Chem. **94**, 6341 (1990).

[5] B. M. Toselli, J. D. Brenner, M. L. Yerram, W. E. Chin, K. D. King, and J. R. Barker, J. Chem. Phys. **95**, 176 (1991).

[6] B. M. Toselli and J. R. Barker (manuscriptt in preparation).

[7] B. M. Toselli, T. L. Walunas, and J. R. Barker, J. Chem. Phys. **92**, 4793 (1990).

[8] H. Hippler, L. Lindemann, and J. Troe, J. Chem. Phys. **83**, 3906 (1985); H. Hippler, B. Otto, and J. Troe, Ber. Bunsenges. Phys. Chem. **93**, 428 (1989).

[9] H. Hippler, J. Troe, and J. Wendelken, J. Chem. Phys. **78**, 6709 (1983); **78**, 6718 (1983).

[10] M. Heymann, H. Hippler, D. Nahr, H. J. Plach, and J. Troe, J. Phys. Chem. **92**, 5507 (1988).

[11] J. E. Dove, H. Hippler, and J. Troe, J. Chem. Phys. **82**, 1907 (1985); M. Heymann, H. Hippler, H. J. Plach, and J. Troe, *ibid.* **87**, 3867 (1987).

[12] M. Damm, F. Deckert, H. Hippler, and J. Troe, J. Phys. Chem. **95**, 2005 (1991).

[13] W. Jalenak, R. E. Weston, Jr., T. J. Sears, and G. W. Flynn, J. Chem. Phys. **89**, 2015 (1988).

[14] J. Z. Chou, S. A. Hewitt, J. F. Hershberger, B. B. Brady, G. B. Spector, L. Chia, and G. W. Flynn, J. Chem. Phys. **91**, 5392 (1989); J. Z. Chou, S. A. Hewitt, J. F. Hershberger, and G. W. Flynn, *ibid.* **93**, 8474 (1990).

[15] J. R. Barker, M. J. Rossi, and J. R. Pladziewicz, Chem. Phys. Lett. **90**, 99 (1982).

[16] A. J. Sedlacek, R. E. Weston, and G. W. Flynn, J. Chem. Phys. **94**, 6483 (1991).

[17] R. K. Huddleston, G. T. Fujimoto, and E. Weitz, J. Chem. Phys. **76**, 3839 (1982).

[18] J. F. Durana and J. D. McDonald, J. Chem. Phys. **64**, 2518 (1976).

[19] R. H. Page, R. H. Shen, and Y. T. Lee, J. Chem. Phys. **88**, 5362 (1988).

[20] J. A. Draeger, Spectrochim. Acta **41**, (1985) 607; H. D. Rudolph, H. Dreizler, A. Jauschke, and P. Wendling, Z. Naturforsch. **22**, 940 (1967).

[21] N. Fuson, C. Garrigou-Lagrange, and M. L. Josien, Spectrochim. Acta **16**, 106 (1960).

[22] T. Shimanouchi, *Tables of Molecular Vibrational Frequencies*, (U.S. GPO, Washington, D.C., 1972), Vol. I.

[23] P. R. Bevington, *Data Reduction and Error Analysis for the Physical Sciences* (McGraw-Hill, New York, 1969), p. 237.

[24] D. M. Bishop and L. M. Cheung, J. Phys. Chem. Ref. Data **11**, 119 (1982).

[25] J. T. Yardley, *Introduction to Molecular Energy Transfer* (Academic, New York, 1980).

[26] B. H. Mahan, J. Chem. Phys. **46**, 98 (1967).

[27] T. A. Dillon and J. C. Stephenson, J. Chem. Phys. **58**, 2056 (1973).

[28] T. Förster, Mod. Quantum Chem. **3**, 93 (1965).

[29] R. D. Sharma and C. A. Brau, J. Chem. Phys. **50**, 924 (1969).

[30] J. C. Stephenson, R. E. Wood, and C. B. Moore, J. Chem. Phys. **48**, 4790 (1968).

[31] R. E. Smalley, Annu. Rev. Phys. Chem. **34**, 129 (1983).

[32] C. Camy Peyret and J. M. Flaud, in *Molecular Spectroscopy: Modern Research*, edited by K. Nakahari Rao (Academic, Orlando, FL, 1985), Vol. III.

[33] Provided by T. J. Wallington (private communication).

[34] K. F. Lim and R. G. Gilbert, J. Phys. Chem. **94**, 72 (1990); **94**, 77 (1990).

[35] M. Bruehl and G. C. Schatz, J. Chem. Phys. **89**, 770 (1988); J. Phys. Chem. **92**, 7223 (1988).

[36] For a recent survey, see R. G. Gilbert and S. C. Smith, *Theory of Unimolecular and Recombination Reactions* (Blackwell, Oxford, 1990), Chap. 5.

[37] J. M. Gomez Llorente, U. Hahn, and H. S. Taylor, J. Chem. Phys. **92**, 2762 (1990).

[38] Y. N. Lin, S. C. Chan, and B. S. Rabinovitch, J. Phys. Chem. **72**, 1932 (1968).

[39] Beatriz M. Toselli and John R. Barker, Chem. Phys. Lett. **174**, 304 (1990).

[40] D. C. Tardy and B. S. Rabinovitch, Chem. Rev. **77**, 369 (1977); M. Quack and J. Troe, *Gas Kinetics and Energy Transfer* (Chemical Society, London, 1977), Vol. 2; H. Hippler and J. Troe, in *Bimolecular Collisions*, edited by J. E. Baggott and M. N. Ashford (The Royal Society of Chemistry, London, 1989), p. 209; I. Oref and D. C. Tardy, Chem. Rev. **90**, 1407 (1990).